Editors' Suggestion

Orientation of the ground-state orbital in $CeCoIn_5$ and $CeRhIn_5$

M. Sundermann,[1,2] A. Amorese,[1,2] F. Strigari,[1,*] B. Leedahl,[2] L. H. Tjeng,[2] M. W. Haverkort,[3] H. Gretarsson,[2,4] H. Yavaş,[2,4,†] M. Moretti Sala,[5,‡] E. D. Bauer,[6] P. F. S. Rosa,[6] J. D. Thompson,[6] and A. Severing[1,2,§]

[1]*Institute of Physics II, University of Cologne, Zülpicher Straße 77, 50937 Cologne, Germany*
[2]*Max Planck Institute for Chemical Physics of Solids, Nöthnitzer Straße 40, 01187 Dresden, Germany*
[3]*Institute for Theoretical Physics, Heidelberg University, Philosophenweg 19, 69120 Heidelberg, Germany*
[4]*PETRA III, Deutsches Elektronen-Synchrotron (DESY), Notkestraße 85, 22607 Hamburg, Germany*
[5]*European Synchrotron Radiation Facility, 71 Avenue des Martyrs, CS40220, F-38043 Grenoble Cedex 9, France*
[6]*Los Alamos National Laboratory, Los Alamos, New Mexico 87545, USA*

(Received 18 February 2019; revised manuscript received 22 May 2019; published 21 June 2019)

We present core level nonresonant inelastic x-ray scattering (NIXS) data of the heavy-fermion compounds $CeCoIn_5$ and $CeRhIn_5$ measured at the Ce $N_{4,5}$ edges. The higher than dipole transitions in NIXS allow determining the orientation of the Γ_7 crystal-field ground-state orbital within the unit cell. The crystal-field parameters of the CeMIn$_5$ compounds and related substitution phase diagrams have been investigated in great detail in the past; however, whether the ground-state wave function is the Γ_7^+ ($x^2 - y^2$) or Γ_7^- (xy orientation) remained undetermined. We show that the Γ_7^- doublet with lobes along the (110) direction forms the ground state in $CeCoIn_5$ and $CeRhIn_5$. For $CeCoIn_5$, however, we find also some contribution of the first excited state crystal-field state in the ground state due to the stronger hybridization of $4f$ and conduction electrons, suggesting a smaller α^2 value than originally anticipated from x-ray absorption. A comparison is made to the results of existing density functional theory plus dynamical mean-field theory calculations.

DOI: 10.1103/PhysRevB.99.235143

I. INTRODUCTION

At high temperature, heavy-fermion materials are described by decoupled localized f electrons and conduction electron bands. Upon cooling, the localized f electrons start to interact with the conduction electrons (cf hybridization) and become partially delocalized. The resulting entangled fluid consists of heavy quasiparticles with masses up to three orders of magnitude larger than the free electron mass. These quasiparticles may undergo magnetic or superconducting transitions. In the Doniach phase diagram temperature T versus exchange interaction $\mathcal{J}$, magnetic order prevails for small $\mathcal{J}$ whereas a nonmagnetic Kondo singlet state forms for large $\mathcal{J}$. Between these two regimes quantum critical behavior occurs which is often accompanied by a superconducting dome that hides a quantum critical point (QCP) [1,2]. Understanding how these quasiparticles, that have atomiclike as well as itinerant character, give rise to these ground states is a challenging question in condensed-matter physics, and the answer to this question will provide a predictive understanding of these quantum states of matter [3].

The tetragonal compounds CeMIn$_5$ (M = Co, Rh, Ir) are heavy-fermion compounds that display different ground states for different transition-metal ions; for M = Co and Ir the ground state is superconducting (T_c = 2.3 and 0.4 K) and for M = Rh it is antiferromagnetic (T_N = 3.8 K) [4]. High-quality CeMIn$_5$ crystals can be grown, making this family suitable for determining the parameter that drives the different ground states. Within the above-mentioned extended Doniach phase diagram, $CeRhIn_5$ is on the weak side of hybridization, $CeCoIn_5$ close to the QCP, and $CeIrIn_5$ is on the side of stronger cf hybridization, i.e., superconductivity goes along with stronger cf hybridization. Although there are strong indications for localization (Rh) and delocalization (Co,Ir) in, e.g., the size of the Fermi surface [5–12], it is not possible to detect the differences in f occupations. They are so subtle that they are below the detection limit [13].

A light-polarization analysis of soft x-ray absorption spectroscopy (XAS) spectra shows that the crystal-field wave function of the ground state correlates with the ground-state properties in the temperature–transition-metal (substitution) phase diagram of $CeCoIn_5$-$CeRhIn_5$-$CeRh_{1-\delta}Ir_\delta In_5$-$CeIrIn_5$; orbitals more compressed in the tetragonal ab plane favor an antiferromagnetic ground state as for $CeRhIn_5$ and the Rh-rich compounds with $\delta \leqslant 0.2$. The compounds with more elongated orbitals along the c axis, however, have superconducting ground states ($CeCoIn_5$, $CeIrIn_5$, and also the Ir-rich compounds with $\delta \geqslant 0.7$) [14,15]. The obvious conclusion is that the more pronounced extension of the ground-state orbitals in the direction of quantization (crystallographic c direction) promotes stronger hybridization in the z direction and hence superconductivity. This is supported by combined

*Present address: Bundesanstalt für Straßenwesen, Cologne, Germany.
†Present address: SLAC National Accelerator Laboratory, 2575 Sand Hill Rd, Menlo Park, CA 94025, USA.
‡Present address: Dipartimento di Fisica, Politecnico di Milano, Piazza Leonardo da Vinci 32, I-20133 Milano, Italy.
§Corresponding author: severing@ph2.uni-koeln.de

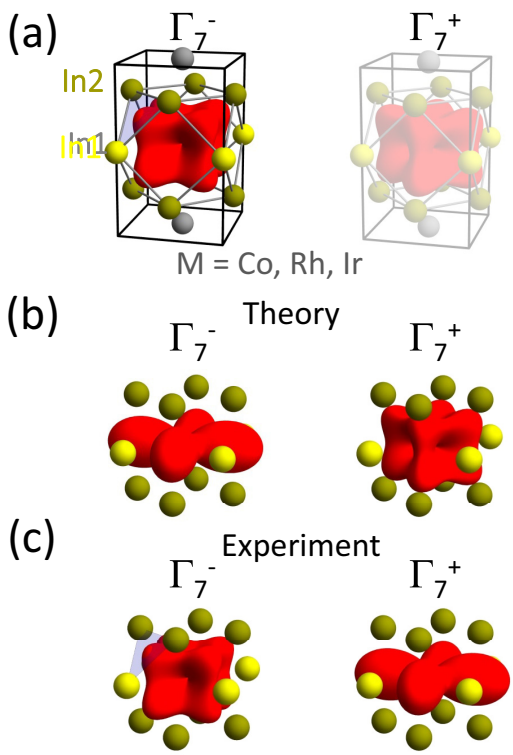

FIG. 1. (a) Cartoon of unit cell of CeMIn$_5$, with orbital shape of Ce in CeCoIn$_5$ as taken from XAS for the possibility of a Γ_7^- and Γ_7^+ Ce ground-state orbital. The light-blue triangle emphasizes the In2-In1-In2 triangle. (b) Weiss field hybridization function for CeMIn$_5$ from DFT + DMFT calculations decomposed into crystal-field components of the Ce ion (red orbitals) and the out-of-plane In2 (dark-yellow dots) and in-plane In1 (yellow dots) environment, adapted from Ref. [19]. (c) Crystal-field components of the Ce ions and environment of In ions as obtained from the present NIXS experiment.

local density approximation plus dynamical mean-field theory (LDA + DMFT) calculations by Shim *et al.* [16] that find for CeIrIn$_5$ the strongest hybridization with the out-of-plane In(2) ions [see unit cell in Fig. 1(a)]. It was also shown that the suppression of superconductivity in CeCo(In$_{1-y}$Sn$_y$)$_5$ by about 3% of Sn is due to a homogeneous increase of hybridization in the tetragonal *ab* plane since the Sn ions go preferably to the In(1) sites [17]. Accordingly, we found that here the hybridization with In(1) ions plays a decisive role; the $4f$ ground-state orbital extends increasingly in the plane as the Sn content is increased [18].

Hence, the ground-state wave function is a very sensitive probe for quantifying hybridization. Haule *et al.* obtained a $4f$ Weiss field hybridization function for CeMIn$_5$ based on realistic lattice parameters using density functional theory plus dynamical mean field (DFT + DMFT) calculations which they have decomposed into crystal-field components [see Fig. 1(b)] [19]. Here our goal is to verify that the crystal-field components that were extracted in these calculations are in agreement with reality.

The tetragonal point symmetry of Ce in CeMIn$_5$ splits the Ce Hund's rule ground state into three Kramers doublets, two Γ_7 doublets $\Gamma_7^{+/-} = |\alpha||\pm 5/2\rangle + / - \sqrt{1-\alpha^2}|\mp 3/2\rangle$ and $\Gamma_7^{-/+} = \sqrt{1-\alpha^2}|\pm 5/2\rangle - / + |\alpha||\mp 3/2\rangle$, and one $\Gamma_6 = |\mp 1/2\rangle$. We write $+/-$ or $-/+$ because the sign has not yet been determined, and this is the scope of the present paper. Γ_6 as a pure J_z state has full rotational symmetry around the quantization axis c but the mixed states have lobes with fourfold rotational symmetry. The magnitude of α describes the shape and aspect ratio of the $\Gamma_7^{+/-}$ orbitals whereas the sign in the wave function determines how the orbitals are oriented within the unit cell; with the lobes along [100] (Γ_7^+: $x^2 - y^2$) or with the lobes along [110] (Γ_7^-: xy).

The crystal-field potential of the CeMIn$_5$ has been determined with inelastic neutron scattering [20,21] and the ground-state wave functions were studied in greater detail with linear polarized soft XAS [15,18,22]. Hence, the crystal-field energy splittings, the sequence of states ($\Gamma_7^{+/-}$, $\Gamma_7^{-/+}$, Γ_6) and also the magnitude of the α^2 values are known (0.13, 0.38, and 0.25 for Co, Rh, and Ir). Only the sign of the wave function remains unknown because it cannot be determined with any of these dipole-selection-rule based spectroscopies. We therefore set up an experiment to determine the sign of the ground-state wave function in the CeMIn$_5$ compounds in order to find out which one of the two scenarios in Fig. 1(a) applies.

II. METHOD

We performed a core level nonresonant inelastic x-ray scattering (NIXS) experiment at the Ce $N_{4,5}$ edges ($4d \rightarrow 4f$). It has been shown previously that this method is able to detect anisotropies with higher than twofold rotational symmetry [23–28]. In the following, we briefly recap the principles of NIXS, a photon-in photon-out technique with hard x rays ($E_{\text{in}} \approx 10$ keV). Because of the high incident energies, NIXS is bulk sensitive and allows one to reach large momentum transfers $|\vec{q}|$ of the order of 10 Å^{-1} when measuring in backscattering geometry. At such large momentum transfers, the transition operator in the scattering function $S(\vec{q}, \omega)$ can no longer be truncated after the dipole term. As a result, higher order scattering terms contribute to the scattering intensity [23,24,29–33]. For a Ce $4d \rightarrow 4f$ transition at about 10 Å^{-1}, octupole (rank $k = 3$) and triacontadipole ($k = 5$) terms dominate the scattering intensity whereas the dipole part ($k = 1$) is less prominent. Accordingly, the directional dependence of the scattering function in a single crystal experiment follows multipole selection rules, in analogy to the dipole selection rules in linearly polarized XAS. Thus single crystal NIXS yields information not only about the orbital occupation but also the sign of the wave function that distinguishes the xy and $x^2 - y^2$ orientations of a Γ_7 when comparing two directions within the xy plane; here [100] and [110].

III. EXPERIMENT

CeCoIn$_5$ and CeRhIn$_5$ single crystals were grown using the standard In-flux technique. CeCoIn$_5$ crystals are platelike with the [001] direction perpendicular to the plate, whereas CeRhIn$_5$ crystals are more three dimensional. A very detailed structural investigation on the 115 compounds shows that more than 98% of the crystal volumes form in the HoCoGa$_5$

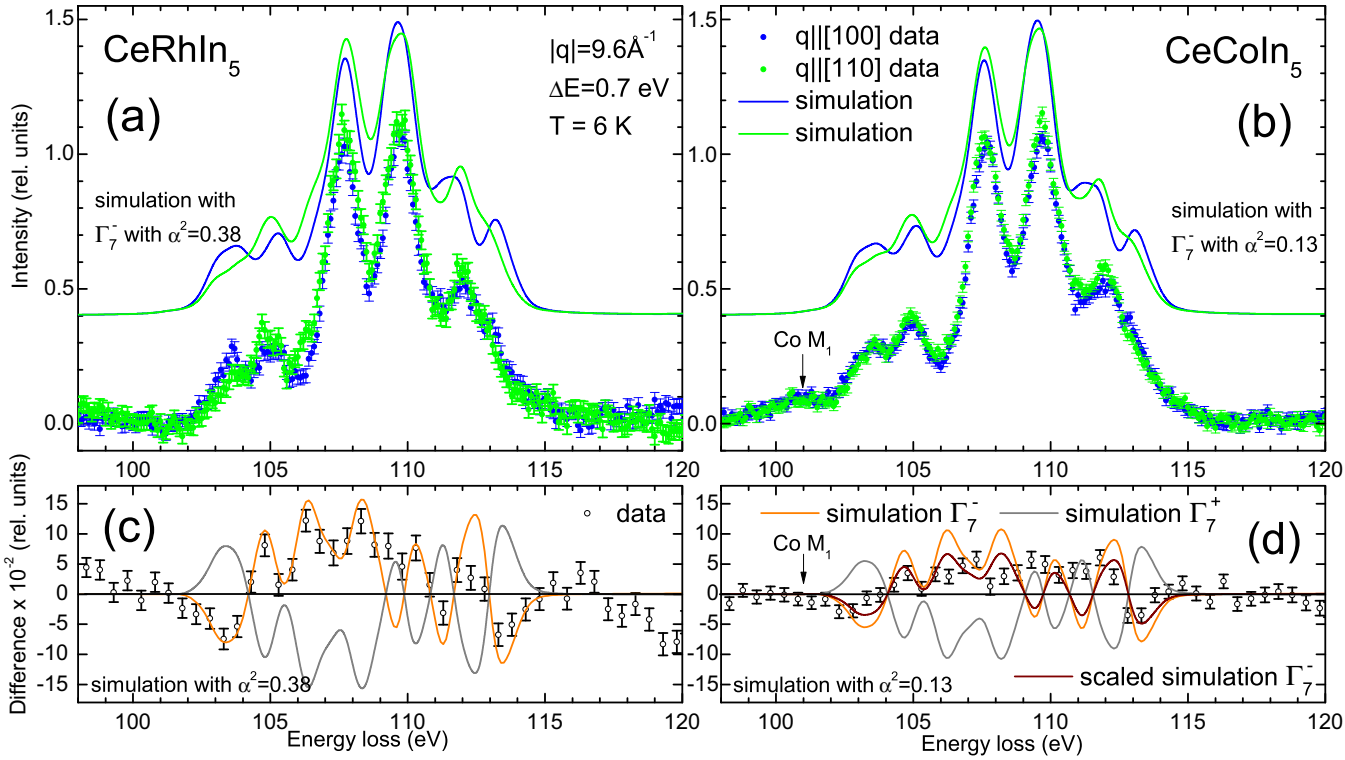

FIG. 2. Nonresonant inelastic x-ray scattering (NIXS) data (dots) of CeRhIn5 (a) and CeCoIn5 (b) at the Ce $N_{4,5}$ edges for the two crystallographic directions $\vec{q} \parallel [100]$ (blue) and $\vec{q} \parallel [110]$ (green) at $T = 6$ K, plus simulations (lines) for the respective Γ_7^- ground states (xy orientation) (see text). The bottom panels (c) and (d) show the difference spectra $I_{\vec{q}\parallel[110]} - I_{\vec{q}\parallel[100]}$ (circles) and simulated dichroism for the respective Γ_7^- (orange lines) and Γ_7^+ (gray lines) crystal-field ground states, and for a mixed ground state called *scaled* Γ_7^- (dark red lines) (see text).

structure [34]. All samples were aligned by Laue diffraction before the experiment. For each compound two samples were cut, one with a (100) and a second one with a (110) surface so that specular geometry could be realized in the experiment.

The experiments were performed at the Max-Planck NIXS end station P01 at PETRA III/DESY in Hamburg, Germany. P01 has a vertical scattering geometry and the incident energy was selected with a Si(311) double monochromator and 12 Si(660) 1 m radius spherically bent crystal analyzers were arranged in 3×4 array as shown in Fig. 2 of Ref. [26] so that the fixed final energy was $E_{\text{final}} = 9690$ eV. The analyzers were positioned at scattering angles of $2\theta \approx 150°$, 155°, and 160° which provide an averaged momentum transfer of $|\vec{q}| = 9.6 \pm 0.1$ Å^{-1}. The scattered beam was detected by a position sensitive custom-made detector (LAMBDA), based on a Medipix3 chip detector. The elastic line was consistently measured and a pixelwise calibration yields instrumental energy resolutions of ≈ 0.7 eV full width at half maximum (FWHM). For both samples the $N_{4,5}$ edges were measured with the momentum transfer $\vec{q}$ parallel to [001] and parallel to [110] ($\vec{q} \parallel [001]$ and $\vec{q} \parallel [110]$).

We used the full multiplet code QUANTY [35] for simulating the NIXS data. A Gaussian broadening of 0.7 eV accounts for the instrumental resolution and an additional Lorentzian broadening of 0.4 eV FWHM accounts for lifetime effects. The atomic parameters were taken from the Cowan code [36], whereby the Hartree-Fock values of the Slater integrals were reduced to about 60% for the $4f$-$4f$ and to about 80% for the $4d$-$4f$ Coulomb interactions to reproduce the energy distribution of the multiplet excitations of the Ce $N_{4,5}$ edges. This reduction accounts for configuration interaction processes not included in the Hartree-Fock scheme [37].

IV. RESULTS

Figure 2 shows NIXS data (circles) at the Ce $N_{4,5}$ edges of $CeRhIn_5$ (a) and $CeCoIn_5$ (b) plus simulations (lines) for two scattering directions, $\vec{q} \parallel [100]$ (blue) and $\vec{q} \parallel [110]$ (green). The overall shape of the spectra looks very similar and represents the multipole scattering expected for the Ce $N_{4,5}$ edges [23–26,30]. Figures 2(c) and 2(d) show the directional dependencies $I_{\vec{q}\parallel[110]} - I_{\vec{q}\parallel[100]}$ (dichroism), the experimental data as circles, and simulations for the Γ_7^- and Γ_7^+ as orange and gray lines, respectively. The expected dichroisms for a Γ_7^- and Γ_7^+ ground state are opposite in sign so that the present experiment provides an either-or result which makes the interpretation of the data straightforward.

For $CeRhIn_5$ the $N_{4,5}$ edges in Fig. 2(a) as well as the dichroism in Fig. 2(c) are fairly well reproduced by the simulation with a Γ_7^- ground state (orange line). Here we used the α^2 value of 0.38 as determined with XAS [22]. The same simulation with a Γ_7^+ ground state is clearly in contradiction to the observation (gray line). For $CeCoIn_5$ the agreement between simulated and experimental directional dependence in Fig. 2(d) is not as good, and we will discuss below the possible reasons for this. Also here the simulation

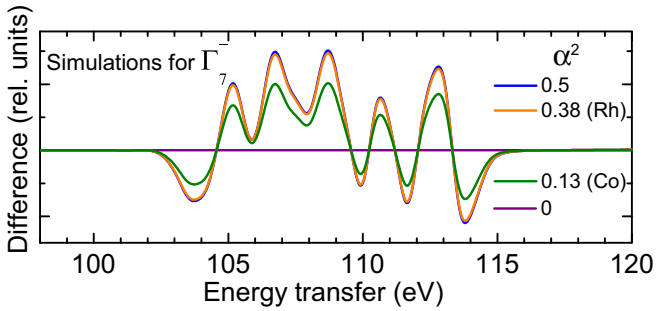

FIG. 3. Simulated difference spectra $I_{\vec{q}\|[110]} - I_{\vec{q}\|[100]}$ for α^2 values of 0 and 0.5, and of 0.38 for $CeRhIn_5$ and 0.13 for $CeCoIn_5$.

was performed with the corresponding α^2 value from XAS, $\alpha^2 = 0.13$ [22]. Most importantly, however, we conclude that the ground state of $CeCoIn_5$ must be also predominantly of Γ_7^- character because the size of the scaling between experiment and calculation is clearly positive (0.63 ± 0.19) [38] and because the Γ_7^+ is, as for $CeRhIn_5$, in clear contradiction to the observation.

V. DISCUSSION

In Fig. 3, we compare the directional dependence $I_{\vec{q}\|[110]} - I_{\vec{q}\|[100]}$ for several α^2 values. For $\alpha^2 = 0$ (or 1) the dichroism is zero because in this case the Γ_7 state is a pure J_z state and rotational invariant; for $\alpha^2 = 0.5$ the dichroism is largest. For $CeRhIn_5$ ($\alpha^2 = 0.38$) the mixing factor α^2 is closer to 0.5 than for $CeCoIn_5$ ($\alpha^2 = 0.13$) so that the expected dichroism for $CeCoIn_5$ is smaller than for $CeRhIn_5$. But, the expected reduction due to the different α^2 values still does not account for the strongly reduced directional effect in $CeCoIn_5$. A natural explanation could be the stronger cf hybridization in $CeCoIn_5$ with respect to $CeRhIn_5$: in $CeCoIn_5$ the coherence temperature T^* is of the order of 50 K [22,39], which is comparable to the energy splitting of the two lowest crystal-field states (6.8 meV or ≈75 K) (see Fig. 4) so that the first excited crystal-field state will contribute to the ground state via hybridization. The first excited crystal-field state is the Γ_7^+ which has the opposite dichroism of the crystal-field ground state Γ_7^- so that the net dichroism of the hybridized ground state will be reduced. In short, the strongly reduced directional effect in $CeCoIn_5$ is due to the presence of strong hybridization. Assuming the first excited crystal-field state Γ_7^+ contributes 19% to the ground state of $CeCoIn_5$ yields a very good agreement of measured dichrosim and simulation [see dark red line in Fig. 2(d)] [38]. However, 19 % of Γ_7^+ mixed into the ground state by hybridization must be an overestimation because the Γ_7^+ admixture was not accounted for when describing the linear dichroism in XAS [22]. It turns out that both data sets, the directional dependence in NIXS and the linear dichroism in XAS, can be analyzed consistently and are well described with $\alpha^2 = 0.10$ and 13% of Γ_7^+.

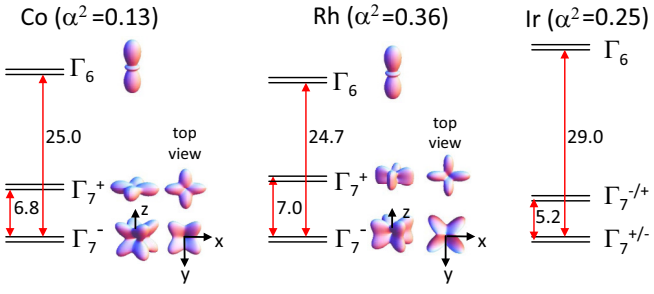

FIG. 4. Crystal-field splitting of $J = 5/2$ multiplet of $CeCoIn_5$, $CeRhIn_5$ and for completeness of $CeIrIn_5$ as adapted from Refs. [20–22]. For M = Co and Rh the sign of the wave function is now determined which has been taken into account when drawing the f^1 charge densities of the respective states.

Figure 4 summarizes what we know now about the crystal-field splittings of the $J = 5/2$ multiplet of $CeMIn_5$. The splittings and α^2 values are taken from inelastic neutron scattering and XAS as published in Refs. [20–22]. The present NIXS experiments on $CeCoIn_5$ and $CeRhIn_5$ add the missing information that the Γ_7^- dominates the ground state for both compounds, i.e., the lobes of the crystal-field ground state are along the crystallographic (110) direction. These Γ_7^- ground state orbitals extend more in the z direction than the Γ_7^+ at about 6–7 meV so that the scenario as shown in Fig. 1(c) applies to $CeCoIn_5$ and $CeRhIn_5$, whereas the wave functions projected out by DFT + DMFT calculations [19] have opposite signs [see Fig. 1(b)].

The tips of the lobes of the Γ_7^- ground-state wave functions of $CeCoIn_5$ and $CeRhIn_5$ are pointing toward the triangle In2-In1-In2 [see Fig. 1(c)]. It is therefore reasonable to conclude that the impact of the hybridization with the out-of-plane In2 atoms is more important than the hybridization with the in-plane In1 atoms. This is in agreement with the results of the $CeRh_{1-\delta}Ir_\delta In_5$ substitution series [15] where the orbitals that are more extended along the c axis tend to hybridize more strongly. Nevertheless, the present results also show that hybridization with the In1 atoms is important and this supports the results of the $CeCo(In_{1-y}Sn_y)_5$ substitution series [18]; the Sn atoms go preferably to the In1 sites leading to a stronger hybridization in the plane [17]. We would like to note that the revised value of α^2 for $CeCoIn_5$ that is obtained when taking into account the first excited crystal-field state leads to a crystal-field ground-state orbital that is even more extended in the z direction than for the originally anticipated value. The same should apply to $CeIrIn_5$ when allowing a hybridization-induced contribution of the first excited crystal-field state. Hence, the correlation of stronger hybridization with the In2 atoms due to ground-state orbitals that are more extended in the z direction and superconductivity still holds [15].

A modest increase in the contribution of $J_z = |\pm 5/2\rangle$ to the Γ_7^- state of $CeRhIn_5$ will promote overlap of f orbitals with p states of In(1) at the expense f-In(2) hybridization. Mixing of Zeeman-split ground and Γ_7^+ first excited crystal-field levels, in principle, could produce such a modest increase in the $J_z = |\pm 5/2\rangle$ contribution. Indeed, recent high-field magnetostriction [40] and nuclear magnetic resonance [41] measurements on $CeRhIn_5$ are consistent with this possibility that appears to be a significant contributing factor to field-induced Fermi-surface reconstruction in $CeRhIn_5$ subject to a magnetic field near 30 T.

In the limit of strong intra-atomic Coulomb interactions, which is typical of strongly correlated metals such as $CeCoIn_5$ and $CeRhIn_5$, the magnetic exchange $\mathcal{J}$ is proportional to the square of the matrix element $\langle V_{kf}\rangle$ that mixes conduction and f wave functions [42]. Both Kondo and long-range Ruderman-Kittel-Kasuya-Yosida interactions depend on the magnitude of $\mathcal{J}$ that is set by $\langle V_{kf}\rangle^2$ and, consequently, by the f-orbital configuration. These interactions are fundamental for a description of Kondo-lattice systems and their relative balance can be tuned by nonthermal control parameters, such as magnetic field and pressure. Modest pressure applied to $CeRhIn_5$ tunes its antiferromagnetic transition temperature toward zero temperature where a dome of unconventional superconductivity emerges with a maximum transition temperature very close to that of $CeCoIn_5$ [4] and also changes the Fermi surface from small to large as in $CeCoIn_5$ [8]. We do not know if the f-orbital configuration of $CeRhIn_5$ at these pressures is the same as that of $CeCoIn_5$, but this is an interesting possibility that merits study.

VI. SUMMARY

In f-based materials, the shape of the crystal-field wave functions ultimately determines the origin of anisotropic hybridization in these materials and their ground state. Here, we show that the ground state of $CeRhIn_5$ is well described by the $\Gamma_7^- = |\alpha||\pm 5/2\rangle - \sqrt{1-\alpha^2}|\mp 3/2\rangle$ doublet with lobes Γ_7^- pointing toward the 110 direction, i.e., the lobes have xy character. The same is valid for $CeCoIn_5$ although we find here some contribution of the first excited crystal-field state in the more strongly hybridized ground state. 13% of the first excited crystal-field state and an adjusted α^2 value of 0.1 describe NIXS and XAS data of $CeCoIn_5$ consistently. Although careful DFT + DMFT calculations shed light on these materials, the crystal-field scheme obtained is different from our experimental one. Our work settles the question on the orientation of f orbitals in the ground state of $CeMIn_5$ and will stimulate theoretical developments that take into account the actual wave functions.

ACKNOWLEDGMENTS

We thank Peter Thalmeier for fruitful discussions. Parts of this research were carried out at PETRA III/DESY, a member of the Helmholtz Association HGF, and we would like to thank Christoph Becker, Manuel Harder, and Frank-Uwe Dill for skillful technical assistance. Work at Los Alamos was performed under the auspices of the U.S. Department of Energy, Office of Basic Energy Sciences, Division of Materials Science and Engineering. A.A., A.S., and M.S. gratefully acknowledge the financial support of the Deutsche Forschungsgemeinschaft under project SE 1441-4-1.

[1] H. v. Löhneysen, A. Rosch, M. Vojta, and P. Wölfle, Fermi-liquid instabilities at magnetic quantum phase transitions, Rev. Mod. Phys. **79**, 1015 (2007).

[2] S. Wirth and F. Steglich, Exploring heavy fermions from macroscopic to microscopic length scales, Nat. Rev. Mater. **1**, 16066 (2016).

[3] P. Coleman, *Handbook of magnetism and magnetic materials*, in *Heavy fermions: Electrons at the edge of magnetism*, edited by H. Kronmüller, S. Parkin, M. Fähnle, S. Maekawa, and I. Zutic (Wiley, New York, 2007), Vol. 1, pp. 95.

[4] J. D. Thompson and Z. Fisk, Progress in heavy-fermion superconductivity: Ce115 and related materials, J. Phys. Soc. Jpn. **81**, 011002 (2012).

[5] Y. Haga, Y. Inada, H. Harima, K. Oikawa, M. Murakawa, H. Nakawaki, Y. Tokiwa, D. Aoki, H. Shishido, S. Ikeda, N. Watanabe, and Y. Onuki, Quasi-two-dimensional Fermi surfaces of the heavy fermion superconductor $CeIrIn_5$, Phys. Rev. B **63**, 060503(R) (2001).

[6] S.-I. Fujimori, T. Okane, J. Okamoto, K. Mamiya, Y. Muramatsu, A. Fujimori, H. Harima, D. Aoki, S. Ikeda, H. Shishido, Y. Tokiwa, Y. Haga, and Y. Onuki, Nearly localized nature of f electrons in $CeTIn_5$ (T = Rh, Ir), Phys. Rev. B **67**, 144507 (2003).

[7] N. Harrison, U. Alver, R. G. Goodrich, I. Vekhter, J. L. Sarrao, P. G. Pagliuso, N. O. Moreno, L. Balicas, Z. Fisk, D. Hall, Robin T. Macaluso, and Julia Y. Chan, $4f$-Electron Localization in $Ce_xLa_{1-x}MIn_5$ with M = Co, Rh, or Ir, Phys. Rev. Lett. **93**, 186405 (2004).

[8] H. Shishido, R. Settai, H. Harima, and Y. Onuki, A drastic change of the Fermi surface at a critical pressure in $CeRhIn_5$: dHvA study under pressure, J. Phys. Soc. Jpn. **74**, 1103 (2005).

[9] R. Settai, T. Takeuchi, and Y. Onuki, Recent advances in Ce-based heavy fermion superconductivity and Fermi surface properties, J. Phys. Soc. Jpn. **76**, 051003 (2007).

[10] H. Shishido, R. Settai, T. Kawai, H. Harima, and Y. Onuki, de Haas–van Alphen effect of $CeIr_{1-x}Rh_xIn_5$, J. Magn. Magn. Mater. **310**, 303 (2007).

[11] Swee K. Goh, J. P. Paglione, M. Sutherland, E. C. T. O'Farrell, C. Bergemann, T. A. Sayles, and M. B. Maple, Fermi-Surface Reconstruction in $CeRh_{1-x}Co_xIn_5$, Phys. Rev. Lett. **101**, 056402 (2008).

[12] M. P. Allen, F. Massee, D. K. Morr, J. Van Dyke, A. W. Rost, A. P. Mackenzie, C. Petrovic, and J. C. Davis, Imaging Cooper pairing of heavy fermions in $CeCoIn_5$, Nat. Phys. **9**, 468 (2013).

[13] M. Sundermann, F. Strigari, T. Willers, J. Weinen, Y. F. Liao, K.-D. Tsuei, N. Hiraoka, H. Ishii, H. Yamaoka, J. Mizuki, Y. Zekko, E. D. Bauer, J. L. Sarrao, J. D. Thompson, P. Lejay, Y. Muro, K. Yutani, T. Takabatake, A. Tanaka, N. Hollmann, L. H. Tjeng, and A. Severing, Quantitative study of the f occupation in $CeMIn_5$ and other cerium compounds with hard x-rays, J. Electron. Spectrosc. Relat. Phenom. **209**, 1 (2016).

[14] P. G. Pagliuso, R. Movshovich, A. D. Bianchi, M. Nicklas, N. O. Moreno, J. D. Thompson, M. F. Hundley, J. L. Sarrao, and Z. Fisk, Multiple phase transitions in Ce(Rh, Ir, Co)In_5, Physica B **312–313**, 129 (2002).

[15] T. Willers, F. Strigari, Z. Hu, V. Sessi, N. B. Brookes, E. D.

Bauer, J. L. Sarrao, J. D. Thompson, A. Tanaka, S. Wirth, L. H. Tjeng, and A. Severing, Correlation between ground state and orbital anisotropy in heavy fermion materials, Proc. Natl. Acad. Sci. USA **112**, 2384 (2015).

[16] J. H. Shim, K. Haule, and G. Kotliar, Modeling the localized-to-itinerant electronic transition in the heavy fermion system $CeIrIn_5$, Science **318**, 1615 (2007).

[17] H. Sakai, F. Ronning, J.-X. Zhu, N. Wakeham, H. Yasuoka, Y. Tokunaga, S. Kambe, E. D. Bauer, and J. D. Thompson, Microscopic investigation of electronic inhomogeneity induced by substitutions in a quantum critical metal $CeCoIn_5$, Phys. Rev. B **92**, 121105(R) (2015).

[18] K. Chen, F. Strigari, M. Sundermann, Z. Hu, Z. Fisk, E. D. Bauer, P. F. S. Rosa, J. L. Sarrao, J. D. Thompson, J. Herrero-Martin, E. Pellegrin, D. Betto, K. Kummer, A. Tanaka, S. Wirth, and A. Severing, Evolution of ground-state wave function in $CeCoIn_5$ upon Cd or Sn doping, Phys. Rev. B **97**, 045134 (2018).

[19] K. Haule, C.-H. Yee, and K. Kim, Dynamical mean-field theory within the full-potential methods: Electronic structure of $CeIrIn_5$, $CeCoIn_5$, and $CeRhIn_5$, Phys. Rev. B **81**, 195107 (2010).

[20] A. D. Christianson, J. M. Lawrence, P. G. Pagliuso, N. O. Moreno, J. L. Sarrao, J. D. Thompson, P. S. Riseborough, S. Kern, E. A. Goremychkin, and A. H. Lacerda, Neutron scattering study of crystal fields in $CeRhIn_5$, Phys. Rev. B **66**, 193102 (2002).

[21] A. D. Christianson, E. D. Bauer, J. M. Lawrence, P. S. Riseborough, N. O. Moreno, P. G. Pagliuso, J. L. Sarrao, J. D. Thompson, E. A. Goremychkin, F. R. Trouw, M. P. Hehlen, and R. J. McQueeney, Crystalline electric field effects in $CeMIn_5$ (M=Co,Rh,Ir): Superconductivity and the influence of Kondo spin fluctuations, Phys. Rev. B **70**, 134505 (2004).

[22] T. Willers, Z. Hu, N. Hollmann, P. O. Körner, J. Gegner, T. Burnus, H. Fujiwara, A. Tanaka, D. Schmitz, H. H. Hsieh, H.-J. Lin, C. T. Chen, E. D. Bauer, J. L. Sarrao, E. Goremychkin, M. Koza, L. H. Tjeng, and A. Severing, Crystal-field and Kondo-scale investigations of $CeMIn_5$ (M = Co, Ir, and Rh): A combined x-ray absorption and inelastic neutron scattering study, Phys. Rev. B **81**, 195114 (2010).

[23] R. A. Gordon, M. W. Haverkort, S. Sen Gupta, and G. A. Sawatzky, Orientation-dependent x-ray Raman scattering from cubic crystals: Natural linear dichroism in MnO and CeO_2. J. Phys. Conf. Ser. **190**, 012047 (2009).

[24] T. Willers, F. Strigari, N. Hiraoka, Y. Q. Cai, M. W. Haverkort, K.-D. Tsuei, Y. F. Liao, S. Seiro, C. Geibel, F. Steglich, L. H. Tjeng, and A. Severing, Determining the In-Plane Orientation of the Ground-State Orbital of $CeCu_2Si_2$, Phys. Rev. Lett. **109**, 046401 (2012).

[25] J.-P. Rueff, J. M. Ablett, F. Strigari, M. Deppe, M. W. Haverkort, L. H. Tjeng, and A. Severing, Absence of orbital rotation in superconducting $CeCu_2Ge_2$, Phys. Rev. B **91**, 201108(R) (2015).

[26] M. Sundermann, K. Chen, H. Yavas, Hanoh Lee, Z. Fisk, M. W. Haverkort, L. H. Tjeng, and A. Severing, The quartet ground state in CeB_6: An inelastic x-ray scattering study, Europhys. Lett. **117**, 17003 (2017).

[27] M. Sundermann, H. Yavas, K. Chen, D. J. Kim, Z. Fisk, D. Kasinathan, M. W. Haverkort, P. Thalmeier, A. Severing, and L. H. Tjeng, $4f$ Crystal Field Ground State of the Strongly Correlated Topological Insulator SmB_6, Phys. Rev. Lett. **120**, 016402 (2018).

[28] M. Sundermann, G. van der Laan, A. Severing, L. Simonelli, G. H. Lander, M. W. Haverkort, and R. Caciuffo, Crystal-field states of UO_2 probed by directional dependence of nonresonant inelastic x-ray scattering, Phys. Rev. B **98**, 205108 (2018).

[29] M. W. Haverkort, A. Tanaka, L. H. Tjeng, and G. A. Sawatzky, Nonresonant Inelastic X-Ray Scattering Involving Excitonic Excitations: The Examples of NiO and CoO, Phys. Rev. Lett. **99**, 257401 (2007).

[30] R. A. Gordon, G. T. Seidler, T. T. Fister, M. W. Haverkort, G. A. Sawatzky, A. Tanaka, and T. K. Sham, High multipole transitions in NIXS: Valence and hybridization in 4f systems, Europhys. Lett. **81**, 26004 (2008).

[31] J. A. Bradley, S. Sen Gupta, G. T. Seidler, K. T. Moore, M. W. Haverkort, G. A. Sawatzky, S. D. Conradson, D. L. Clark, S. A. Kozimor, and K. S. Boland, Probing electronic correlations in actinide materials using multipolar transitions, Phys. Rev. B **81**, 193104 (2010).

[32] J. A. Bradley, K. T. Moore, G. van der Laan, J. P. Bradley, and R. A. Gordon, Core and shallow-core d- to f-shell excitations in rare-earth metals, Phys. Rev. B **84**, 205105 (2011).

[33] R. Caciuffo, G. van der Laan, L. Simonelli, T. Vitova, C. Mazzoli, M. A. Denecke, and G. H. Lander, Uranium $5d$-$5f$ electric-multipole transitions probed by nonresonant inelastic x-ray scattering, Phys. Rev. B **81**, 195104 (2010).

[34] S. Wirth, Y. Prots, M. Wedel, S. Ernst, S. Kirchner, Z. Fisk, J. D. Thompson, F. Steglich, and Y. Grin, Structural investigations of $CeIrIn_5$ and $CeCoIn_5$ on macroscopic and atomic length scales, J. Phys. Soc. Jpn. **83**, 061009 (2014).

[35] M. W. Haverkort, *Quanty* for core level spectroscopy - excitons, resonances and band excitations in time and frequency domain, J. Phys.: Conf. Ser. **712**, 012001 (2016).

[36] R. D. Cowan, *The theory of atomic structure and spectra* (University of California Press, Berkeley, 1981).

[37] A. Tanaka and T. Jo, Resonant $3d$, $3p$ and $3s$ photoemission in transition metal oxides predicted at $2p$ threshold, J. Phys. Soc. Jpn. **63**, 2788 (1994).

[38] The values and standard errors of the mean of the experimental dichroism weighted by and normalized to the one of the Γ_7^- simulation amount to (0.60 ± 0.07) and (0.18 ± 0.05) for $CeRhIn_5$ and $CeCoIn_5$, respectively. We can estimate the scaling between experiment and theory from these values by dividing by the Pearson correlation coefficients $c = 0.72$ for $CeRhIn_5$ and 0.28 for $CeCoIn_5$ and obtain (0.83 ± 0.10) for $CeRhIn_5$ and (0.63 ± 0.19) for $CeCoIn_5$.

[39] C. Petrovic, P. G. Pagliuso, M. F. Hundley, R. Movshovich, J. L. Sarrao, J. D. Thompson, Z. Fisk, and P. Monthoux, Heavy-fermion superconductivity in $CeCoIn_5$ at 2.3 K, J. Phys.: Condens. Matter **13**, L337 (2001).

[40] P. F. S. Rosa, S. M. Thomas, F. F. Balakirev, E. D. Bauer, R. M. Fernandes, J. D. Thompson, F. Ronning, and M. Jaime, Enhanced Hybridization Sets the Stage for Electronic Nematicity in $CeRhIn_5$, Phys. Rev. Lett. **122**, 016402 (2019).

[41] G. G. Lesseux, H. Sakai, T. Hattori, Y. Tokunaga, S. Kambe, P. L. Kuhns, A. P. Reyes, J. D. Thompson, P. G. Pagliuso, and R. R. Urbano, Orbitally defined field-induced electronic state in a Kondo lattice, arXiv:1905.02861v2.

[42] J. R. Schrieffer and P. A. Wolff, Relation between the Anderson and Kondo Hamiltonians, Phys. Rev. **149**, 491 (1966).